



OPEN

A single vector system for tunable and homogeneous dual gene expression in *Escherichia coli*

Z. Živič¹, L. Lipoglavšek², J. Lah¹ & S. Hadži¹✉

Expression of recombinant genes can be controlled using inducible promoters. However, the most commonly used IPTG- and arabinose-inducible promoters result in an 'all-or-nothing' response, leading to fully induced and uninduced bacterial subpopulations. Here, we investigate whether appropriate modifications to these promoter systems can be combined into a single vector system, enabling homogenous expression of two genes of interest that can be precisely tuned using inducer concentration. We show that modifications of positive feedback loops related to inducer uptake result in homogeneous gene expression in both the T7 lactose and pBAD arabinose systems. Furthermore, these two modified systems were combined into a single vector, pRAT-sfGFP that provides the desired tunable expression of two genes of interest. Finally, we test this single-vector system as a tool for studying two-component genetic circuits, using toxin-antitoxin modules as model systems. This novel low-copy single vector expression system opens up new possibilities for investigating the function of two-component bacterial genetic circuits.

Keywords Dual tunable gene expression, Two-component genetic circuits, IPTG, Arabinose, HigBA2, Phd/Doc, Toxin-antitoxin

Recombinant gene expression in *Escherichia coli* can be achieved using a diverse set of methods. A preferred choice is controlled gene expression using inducible promoters which are activated by small molecules¹. These include sugars (e.g. lactose, rhamnose, arabinose)², their synthetic analogues (e.g. IPTG)¹, antibiotics (e.g. tetracycline)³, metabolites (e.g. DAPG, vanillic acid)⁴⁻⁶ and signal molecules (e.g. acyl homoserine lactone, cumate, AHL, choline)^{5,7-9}. Protein production can also be controlled at the translation level using riboswitches that respond to different metabolites (e.g. adenine, guanine)^{10,11} or their synthetic analogues (e.g. ammeline)¹². Although high levels of gene expression are most commonly desired, there are advantages to lowering the rate of protein production and fine-tuning the expression level¹³⁻¹⁵. For example, in the case of large-scale protein production, lowering expression rates can reduce the metabolic burden leading to an increase in overall protein yield¹⁴. Lowering expression rates can also alleviate formation of inclusion bodies¹⁵ and can help with expression of toxic proteins¹⁶. For membrane proteins it also provides more time for protein translocation and can result in an overall higher protein yield¹⁷. Adjustable cell-level expression control is also essential for studying function of genetic circuits *in vivo*.¹⁸

For several promoter systems the expression level can be tuned using inducer concentration, as for example in those induced by tetracycline³ and several sugar metabolism genes induced by D-lactose, D-galactose, N-acetylglucosamine and N-acetylmuramic acid¹⁸. However, the most commonly used IPTG- and arabinose-inducible promoter systems are well-known for their 'all-or-nothing' response¹⁹⁻²¹, characterized by non-homogenous, bimodal gene expression. One explanation of this phenomenon suggests that this is due to the positive feedback loop related to transport of the inducer. Namely, the lactose transporter LacY is positively regulated by its inducer and the positive feedback loop leads to the accumulation of inducer molecules in a subpopulation of cells²¹⁻²⁴. Not only does this lead to non-uniform expression at the population level, but also at the cellular level the expression does not quantitatively depend on the concentration of inducer i.e. it is not tunable. A similar situation occurs for arabinose due to the positive feedback with its own transporter^{25,26}.

Different approaches were developed to rectify the 'all-or-nothing' response in these systems in order to achieve more homogeneous gene expression in the bacterial population. One strategy is to address the problem at its source and disrupt the positive feedback loops related to the inducer transport. For example, constitutive expression of low-affinity high capacity arabinose transporter AraE has resulted in a more even distribution

¹Department of Physical Chemistry, Faculty of Chemistry and Chemical Technology, University of Ljubljana, Ljubljana, Slovenia. ²Chair of Microbial Diversity, Microbiomics and Biotechnology, Biotechnical Faculty, University of Ljubljana, Groblje, Slovenia. ✉email: san.hadzi@fkkt.uni-lj.si

of inducer in the cell population, leading to homogeneous gene expression²⁷. In the case of IPTG-inducible promoter, removal of LacY resulted in homogeneous gene expression²⁸. When the active transport (LacY) is disrupted, the inducer uptake occurs only through passive diffusion, which ensures more even inducer distribution in the cell population and tunable expression²⁸. Mapping of the sugar utilization genes in *E. Coli* revealed that in addition to the inducible transport, sugar catabolism is another mechanism that defines whether a system has a tunable or an ‘all-or-nothing’ response^{2,29}. For this reason, other strategies to improve tunability were also explored. In one example tunable arabinose-induced expression was achieved with growth in a mixed feed environment (D-glucose and L-arabinose)³⁰. A different strategy is used in the Lemo21(DE3) strain, where the T7 RNA polymerase activity is controlled by varying the expression level of its inhibitor LysY thorough the inducible rhamnose promoter³¹. Similarly, adjusting the levels of LacI repressor using inducible rhamnose promoter was also shown to enable tunable IPTG gene expression³². IPTG-induced expression can also be combined with riboswitches in a layered and stringently controlled tunable system³³. Another innovative strategy to achieve homogenous gene expression is to rewire the gene circuit and include an additional negative feedback loop controlling repressor. For example, the tetracycline-induced gene expression changes from bimodal to unimodal when TetR repressor is placed under negative autoregulation³⁴. This modification linearizes inducer dose-response, reduces expression noise and can be utilized also in yeast and mammalian cells^{35,36}. Collectively, several strategies have been developed to modify individual promoters to achieve homogeneous gene expression in bacteria.

For some applications co-expression of two or more genes in a controlled manner is required, for example to efficiently stimulate the formation of multi-subunit complexes (e.g. pETDuet from Novagen) or to study multi-input gene regulatory circuits¹⁸. One type of such a system is a single-vector dual expression system based on the translational control of gene expression via riboswitches. It involves the use of the *addA* riboswitch and its mutant M6 which can be regulated using 2-aminopurine and ammeline in a dose dependent manner, respectively^{12,37}. Another type of a dual expression system is based on the use of two high- and low-copy number vectors with AHL and arabinose as inducers feeding into complex biological circuitry³⁸. IPTG- and tetracycline-induced promoters have also shown promise when combined in a dual expression system, this time once again on two separate vectors³⁹. Dual expression system pdMAX is based on arabinose and IPTG induction, however it lacks the necessary adjustments required for tunable gene expression and dual promoter activity is achieved at low temperatures (16 °C) over a two day incubation period⁴⁰. A set of *E. coli* cells called “Marionette” strains has also been optimized for low cross-talk between a set of 12 small-molecule inducers and allows for > 100-fold induction⁵.

In our work, we aspired to design a system which would enable quantitative titration of two proteins and adjust their ratio by changing inducer concentration, allowing characterization of various two-component genetic circuits. To simplify workflow, we chose to base our design on a low-copy number vector, rather than using genomic alteration of the host cell. Typically, the main focus in characterizing inducible systems is the dynamic range and background expression level, while response homogeneity at the population-level is less characterized, particularly for the combination of several expression systems. Here we focus on the two well-characterized expression systems, T7 lactose and pBAD arabinose, and investigate whether they can be employed together for tunable and unimodal population-wide expression of two genes of interest. We show that with appropriate modifications this system can give > 90% homogenous and tunable expression without significant cross-talk between inducers. Finally, we apply a novel single-vector dual gene expression system, pRAT-sfGFP, to characterize a two-component gene circuit, thereby expanding the genetic toolkit for studying regulatory genetic circuits *in vivo*.

Results and discussion

Tunable and population-wide homogeneous expression using IPTG and arabinose induction

In the standard implementation of the IPTG- and arabinose-inducible promoters, an ‘all-or-nothing’ response is expected and, depending on the inducer concentration, leads to separate induced and uninduced bacterial subpopulations^{19–21}. To investigate whether the arabinose system can be utilized for homogeneous and tunable expression on a low-copy number vector, we designed the vector sfGFP-A (Table S1). The vector consists of the Superfolder GFP (sfGFP) as a reporter protein placed under control of the arabinose promoter P_{BAD} . Additionally, it also contains AraC repressor and AraE transporter genes under constitutive expression, the latter enabling a more homogenous uptake of arabinose. For the T7 promoter system, we used the vector sfGFP-I (Table S1) consisting of sfGFP placed under T7 promoter with the lactose operator (*lacO*) and a constitutively expressing LacI repressor. To achieve unimodal expression from T7 promoter, vectors were transformed into the Tuner[DE3] strain lacking chromosomally-encoded lactose permease which guarantees a more even distribution of IPTG within the cell population²⁸.

To understand how these modifications affect gene expression we measured sfGFP fluorescence. Cells transformed with the sfGFP-I were incubated at eight concentrations of IPTG (0–10 mM), while for sfGFP-A twelve concentrations of arabinose (0–2 mM) were used. After 3 h sfGFP fluorescence was measured using flow cytometry and also in the 48-well plates using plate reader. Both sfGFP-I and sfGFP-A demonstrated homogeneous expression in cell populations (Fig. 1, Figure S3). Unimodal response to inducer was present in more than $86 \pm 2\%$ (sfGFP-A) and $90.9 \pm 0.6\%$ (sfGFP-I) of measured events in the whole concentration range of inducers. As a control, we tested the sfGFP-A vector lacking the constitutive expression of AraE, termed sfGFP-deltamut. As expected, cells not expressing AraE transporter showed a bimodal response, characterized by two distinct cell populations (induced and uninduced), and a lower inducer sensitivity (arabinose concentration at which expression is induced) (Figure S4).

The mean of sfGFP cell fluorescence increases with inducer concentration and plateaus at about 1 mM for IPTG and arabinose (Fig. 1). An identical expression profile as a function of inducer concentration was also

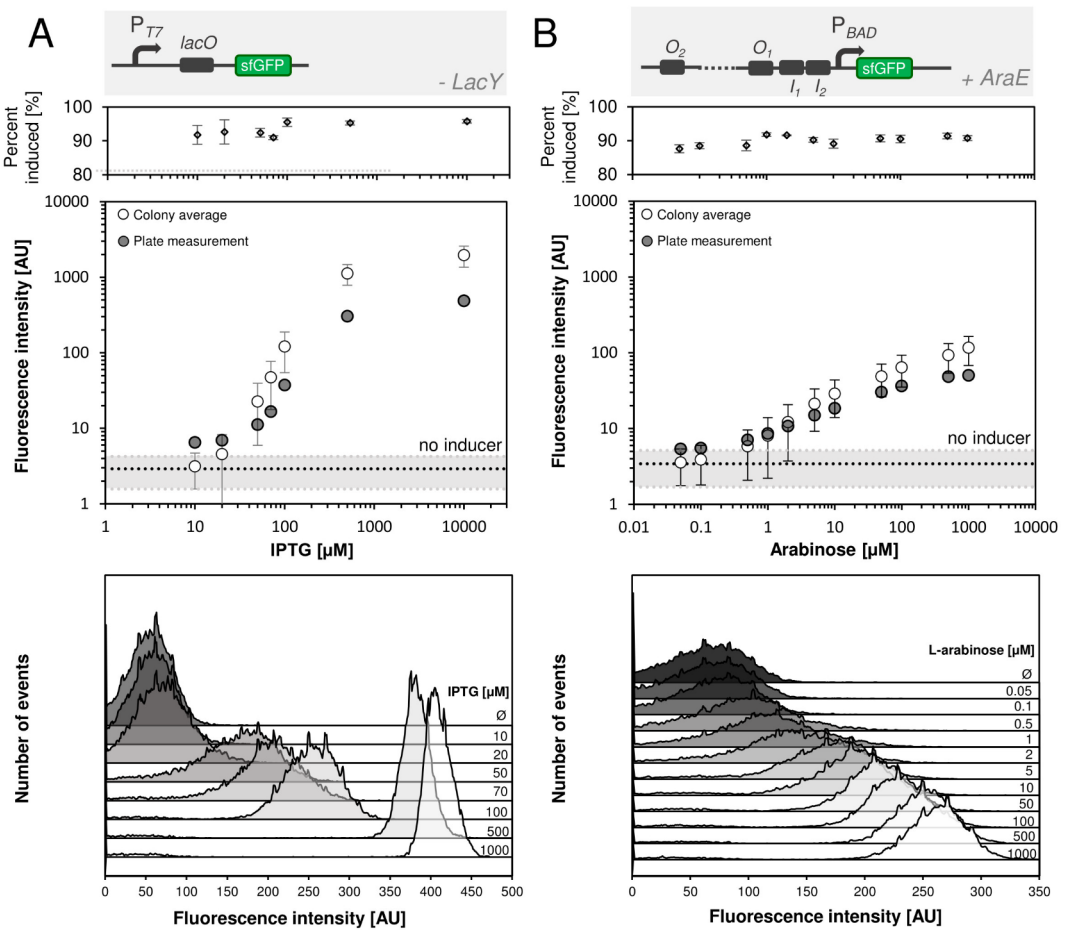


Fig. 1. Population-homogeneous gene expression using IPTG and arabinose. **(A)** Top panel shows the percentage of IPTG-induced sfGFP expression measured using flow cytometry. Middle panel shows fluorescence intensity as a function of inducer concentration for expression of sfGFP in Tuner[DE3] cells measured in plates (black symbols) or by flow cytometry (white symbols, averages of three colonies, error bars indicate standard error of measurement). Bottom panel shows flow cytometry population distribution curves as a function of IPTG concentration for colony 1. **(B)** Percentage of arabinose-induced cells (top panel) and sfGFP fluorescence intensity (middle panel) as a function of arabinose concentration. Cells were either measured directly in plates (black symbols) or using flow cytometry (white symbols). Bottom panel shows the corresponding population distribution curves as a function of arabinose concentration for colony 1.

observed when experiments were performed in bulk 48-well plate format (Fig. 1). Although, the steady state for IPTG-induced sfGFP is reached at around 20 h post-induction, the sfGFP-A fluorescence peaks at 3 h and then drops off significantly (Figure S7), due to arabinose degradation. Therefore, the flow cytometry measurements were performed at 3 h at the peak of arabinose induction. Based on the fluorescence intensity measured with flow cytometer the induction capacity of IPTG is 560 ± 40 -fold at 10 mM three hours post induction, while that of arabinose is weaker up to 46 ± 6 -fold at 2 mM inducer. The observed 46-fold induction by arabinose is lower than the previously reported 1000-fold linear response also containing constitutive AraE expression and the up to 500-fold response in Marionette strains⁵. This is likely explained by longer induction time (more than 5 h vs. 3 h in our experiment). In the first case (1000-fold induction), AraE was constitutively expressed from a low-copy number pJN105 vector, while reporter was present on high-copy number pCSAK50²⁷. In our case both reporter protein and AraE are placed on the same low-copy number vector, likely leading to earlier promoter saturation and lower overall fluorescence. In the case of Marionette strains (500-fold induction), it is notable that optimized mutants of AraC and AraE were used, altering gene expression and inducer sensitivity. Collectively, these results show that the appropriate modifications of the IPTG and arabinose induction systems enable homogeneous gene expression in a bacterial population and tuning of protein induction level expressed from a low-copy number vector.

Arabinose and IPTG exhibit very limited cross-talk

Tunable and homogenous expression of two (or more) genes could be achieved by combining induction systems, provided that that there is no cross-talk between inducers. To investigate the potential cross-talk between IPTG and arabinose we performed expression experiments with sfGFP-I and sfGFP-A in the presence of both inducers

at different concentrations. When sfGFP is induced by IPTG (Fig. 2A, left) addition of arabinose leads to a slight reduction of fluorescence, but at the highest arabinose concentration (500 μ M) an increase of fluorescence intensity is observed. On the other hand, when sfGFP is induced by arabinose (Fig. 2A, right) no changes in fluorescence are observed upon addition of IPTG. To investigate potential inducer cross-talk at the population level we performed flow cytometry measurements. We observed that the fraction of induced cells is not affected by the inducer cross-talk in the range of different inducer concentrations (Fig. 2B, C). For example, when sfGFP-A is induced by 0.1 mM or 1 mM arabinose no interference with IPTG can be observed in terms of the fraction of induced cells and fluorescence intensity (Fig. 2B). Similarly, when sfGFP-I is induced we observed a small decrease with increasing arabinose concentration at 0.04 and 0.05 mM IPTG in bulk measurements. Flow cytometry experiments for sfGFP-I show consistent intensity at 66.6 mM arabinose and only a slight decrease at 666.1 mM arabinose. The overall level of interface between IPTG and arabinose inducers does not seem to significantly affect gene expression.

These findings somewhat deviate from the report by Lee et al. where strong cross-talk between arabinose and IPTG was observed⁴¹. While induction by 10 mM arabinose was not affected by addition of 5 mM IPTG, a dramatic (approximately 7-fold) repression by IPTG was observed when lower concentrations (0.15 mM) of arabinose were used for induction. Meyer et al. also reported that arabinose induction is repressed by 1 mM IPTG, but this effect was much smaller, only about 1.5 fold. In contrast, we did not observe that IPTG represses induction by arabinose (Fig. 2A right, B). Rather, we observe some interference by arabinose when IPTG is used as inducer (Fig. 2A left, C). This could be due to constant AraE expression or the lack of lactose permease, preventing arabinose exclusion and/or IPTG accumulation in cells. In previously reported work, cross-talk is

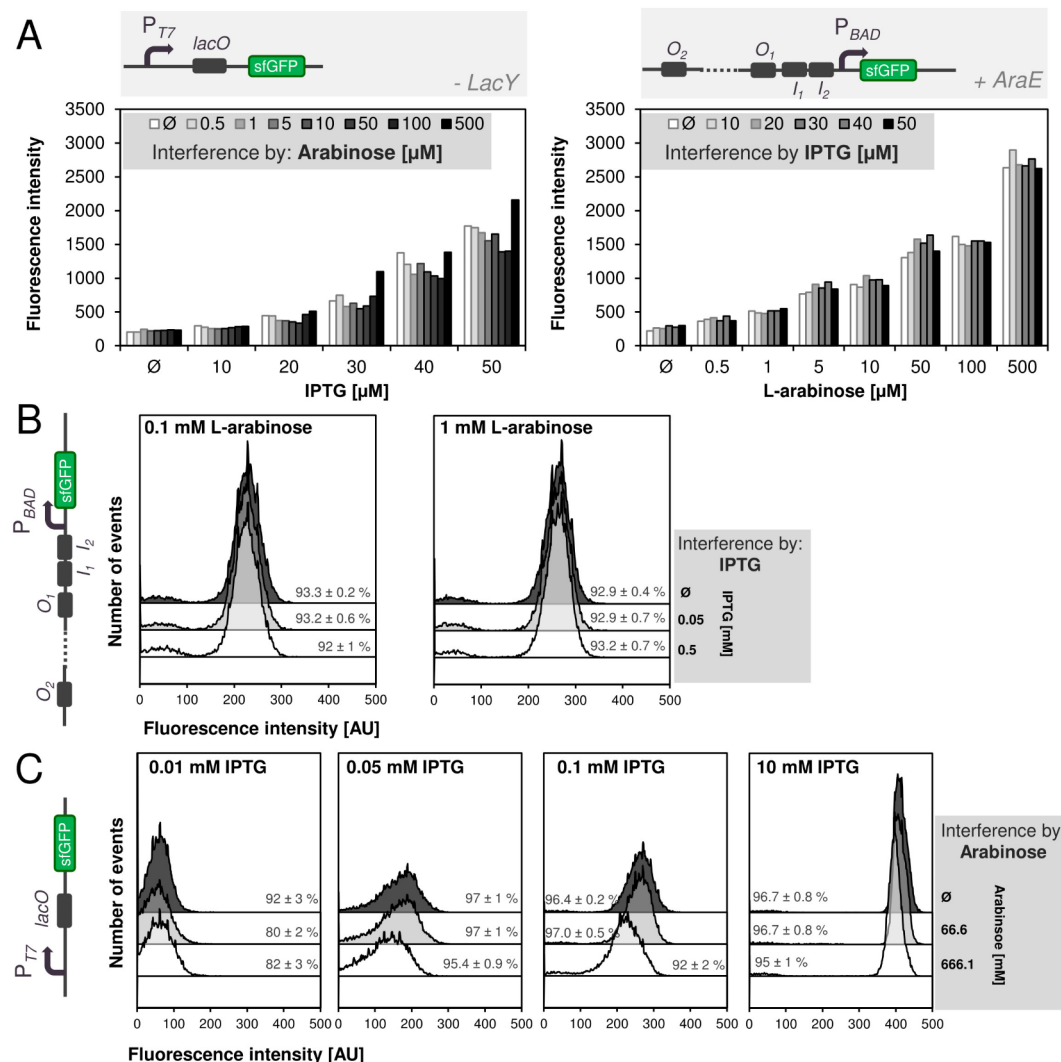


Fig. 2. IPTG and arabinose show no significant cross-talk. (A) sfGFP fluorescence intensity induced by IPTG (left) or arabinose (right) in presence of the second interfering inducer. (B) Population distribution curves for sfGFP induction by 0.1 and 1 mM arabinose (black) in presence of second inducer IPTG (gray, light gray). (C) Population distribution curves for sfGFP induction by 0.01, 0.05, 0.1 and 10 mM IPTG (black) in presence of second inducer arabinose (gray, light gray).

observed in cells which do not metabolize arabinose. The Tuner[DE3] strain used in our work is capable of metabolizing arabinose which might mitigate cross-talk, as arabinose degradation leads to a shorter span of gene expression and therefore less opportunity for cross-talk. Although our work showed no significant cross-talk for sfGFP-A, we further assessed the arabinose-IPTG interference using a modified version of AraC (AraC C280* mutant), which was shown to alleviate the IPTG-arabinose cross-talk⁴¹. However, using AraC C280* mutant we observe practically identical behaviors as with wild-type AraC (Figure S8), in accordance with our results showing the absence of significant crosstalk between two inducers in our system.

Relative gene expression can be tuned by the inducer ratio and relative incubation time

We next determined which expression ratios can be achieved when dual expression with IPTG and arabinose is used. Here we define the expression ratio as the sfGFP fluorescence intensity induced by arabinose (from the sfGFP-A vector) divided by that induced by IPTG (from the sfGFP-I vector). This ratio can be adjusted either inducer concentrations or by expression time, particularly when inducers are not added simultaneously but sequentially. We performed separate experiments with sfGFP-A and sfGFP-I and analyzed the resulting fluorescence ratios (Fig. 3). In the first experiment cells harboring either sfGFP-A or sfGFP-I were grown in separate 48-well plates and induced by a range of combinations of IPTG and arabinose, which were both added at the same time (Fig. 3A, B). The ratio of sfGFP fluorescence from the two plates gives the pBAD vs. T7 expression ratio, which ranges between 1:50 (at 0.5 mM IPTG and 0 mM arabinose) to 5:1 (at 0 mM IPTG and 0.5 mM arabinose) (Fig. 3A). When using a lower range of IPTG concentrations, we observed more comparable gene expressions around 1:5 for both inducers in the 48-combinations of IPTG and arabinose (Fig. 3B). In the third experiment we tested if these expression ratios can be additionally varied by changing the induction time of one of the inducers (Fig. 3C). Again, cells with either sfGFP-A or sfGFP-I were induced with IPTG and arabinose, but IPTG was present in the overnight culture medium, while arabinose was added at time of induction. Although we used same concentration range as in the experiment shown in Fig. 3B, the expression ratios are now very similar as in the experiments shown in Fig. 3A, ranging between 1:50 (at 0.05 mM IPTG and 0 mM arabinose) to 4:1 (at 0 mM IPTG and 0.5 mM arabinose). Therefore, the gene expression ratio can be tuned both by varying the inducer concentrations and by changing the incubation time between the inducers.

The observed expression ratio range appears to be lower than the four magnitudes of expression ratio reported by Daniel et al.³⁸. That system utilizes a combination of two vectors (high and low-copy number) in order to induce the expression of two genes of interest with arabinose and AHL separately. While it offers a wider range of expression ratios, the need for co-transformation of two vectors having separate selection markers can complicate the workflow³⁸. Another previously described dual-tunable expression system based on the translational control using *M6* and *addA* riboswitches allows up to 24-fold induction achieving 5:1–1:5 ratios, which are similar ratios as reported here (Fig. 3B). These expression ratios are close to the typical stoichiometries observed in protein-protein complexes which can be involved in regulation of two-component genetic circuits.

Design of a single-vector system pRAT-sfGFP for homogeneous expression of two genes

Our final aim was to construct a layered single-vector system enabling homogenous and tunable expression of two genes using IPTG and arabinose as inducers. We envisioned that this dual expression system can be used to study regulatory circuits where two proteins (transcription factors or cofactors) regulate the transcription from the promoter of interest. The scaffold vector plasmid for ratio-dependent control of sfGFP expression (named pRAT-sfGFP) (Fig. 4A, Table S1, full sequence in supplementary) includes 2 pairs of homology regions (HR3-6) intended for cloning genes (transcription factors) under the T7 *lacO* or pBAD promoter. The third pair of homology regions (HR1-2) is intended for cloning the promoter, which is placed upstream of the sfGFP used as a reporter of the transcription activity. Finally, a fourth pair of homology regions (HR7-8) places transporter AraE on the scaffold vector to achieve homogeneous induction of the arabinose-inducible gene of interest. Alternatively, AraE can be placed on the chromosomal DNA or under control of a different promoter²⁷. Homology regions are intended for Golden Gate cloning using type IIS enzyme *BsaI*. As origin of replication we use the low-copy number ori p15A (~ 14 copies per cell)⁴² to achieve gene expression at close-to physiologically relevant levels.

This vector design enables investigation of protein/protein ratio-dependent regulatory systems, but also temporal monitoring of systems where one gene is expressed constitutively at different concentrations and another is expressed as a “pulse”, given that arabinose is degraded by the cell after some time and gene expression peaks 2–3 h following addition of arabinose (Figure S7).

Application of dual expression system in mapping the response of two-component genetic circuits

We tested whether the designed vector can be used to study the response of two-component bacterial circuits using toxin-antitoxin modules as model systems. Type II toxin-antitoxin (TA) modules are small bacterial operons with complex regulation⁴³. Toxin and antitoxin genes are transcribed as a single bicistronic mRNA and the transcription is usually regulated by both proteins via the TA operator region, which contains the TA promoter and an antitoxin binding site. Antitoxin binds to this operator and acts as negative regulator, while toxin forms a complex with antitoxin and affects its binding to the operator. Toxin can act as co-repressor, activator or both depending on the toxin/antitoxin ratio and on the type of the system⁴³. The TA modules therefore served as perfect model systems for studying regulatory mechanisms of two-component bacterial circuits.

We focused on two well-characterized toxin/antitoxin systems: *higBA2* which is encoded on the *Vibrio cholerae*⁴⁴ chromosome and the *phd/doc* from bacteriophage P1⁴⁵. HigB2 toxin is a ribosome-dependent mRNase^{44,46}. HigB2 is regulated by antitoxin HigA2 which forms a high-affinity protein-protein complex^{47,48}. Antitoxin HigA2 also acts a transcription regulator, while role of HigB2 in transcription regulation is still not

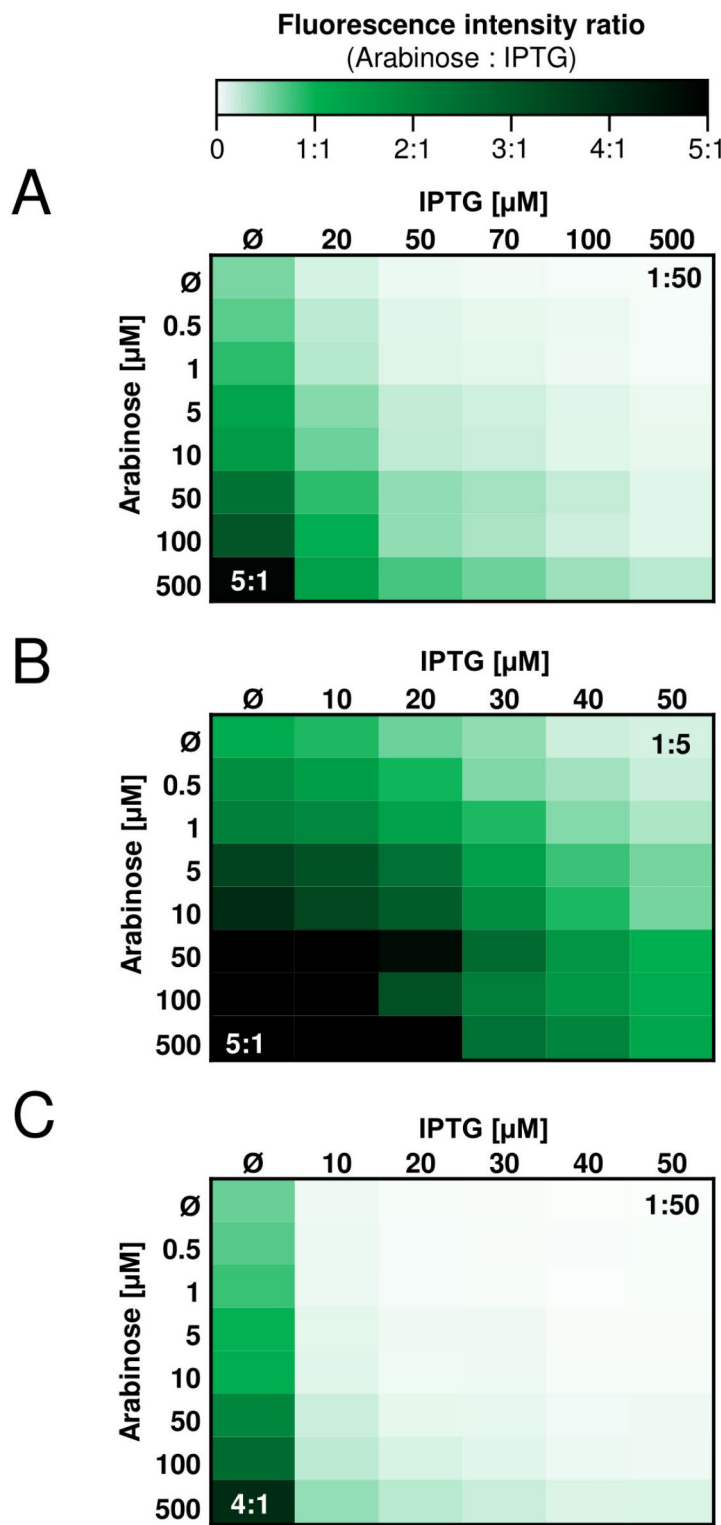


Fig. 3. Different ratios of gene expression can be achieved by varying inducer concentration or induction times. (A, B) Normalized fluorescence ratios for the sfGFP-A/sfGFP-I expression measured separately at 3 h post-induction with both inducers. (C) Normalized fluorescence ratios for the sfGFP-A/sfGFP-I expression measured separately for cells grown overnight in presence of IPTG, while arabinose was induced for 3 h.

known⁴⁹. To study transcription regulation we placed *higBA2* operator region upstream of sfGFP, while antitoxin HigA2 and toxin HigB2 were placed under IPTG-inducible T7 and arabinose-inducible pBAD promoters, respectively. To avoid problems with cell toxicity we used enzymatically inactive HigB2 mutant (R64A, K84A)⁴⁸. The effect of antitoxin on *higBA2* transcription was assessed by measuring sfGFP fluorescence upon addition of

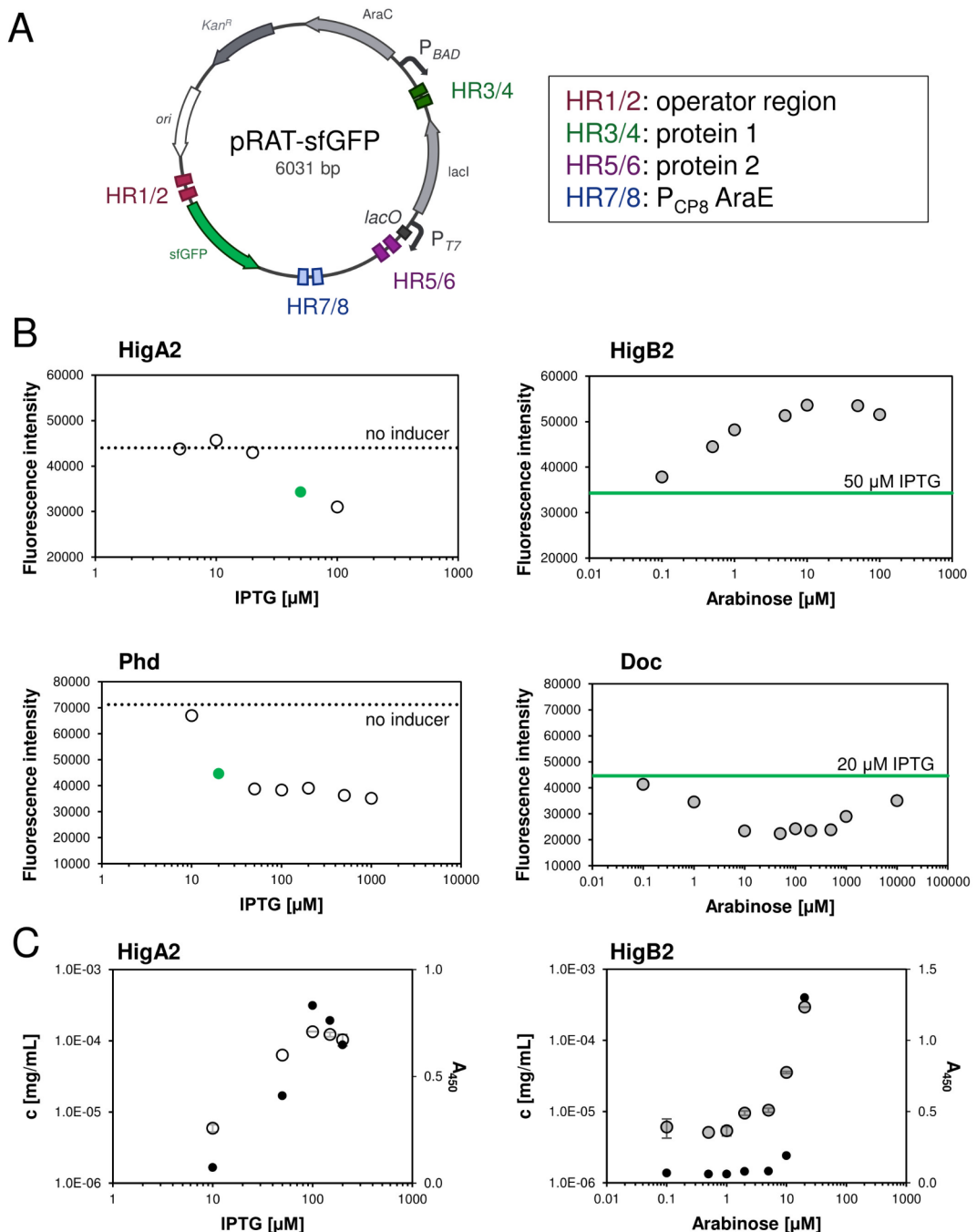


Fig. 4. Design of the pRAT-sfGFP scaffold vector and its application for studying two-component genetic circuits. (A) pRAT-sfGFP vector map shows sites of kanamycin resistance gene (KanR, dark gray), p15A ori (white), repressors lacI and AraC (gray), reporter protein sfGFP (green), arabinose promoter (PBAD), lactose operator (lacO), T7 promoter (PT7) and 4 pairs of homology regions (HR1-8) for Golden Gate cloning using BsaII. (B) Normalized fluorescence measurements of sfGFP upon induction of antitoxin (HigA2, Phd, left) or toxin (HigB2, Doc, right). Values in absence of inducer are indicated as a dotted line (no inducer). Toxin induction was performed in the presence of antitoxin, at the IPTG concentration level resulting in fluorescence values indicated in green (dot/line). (C) Immunodetection using ELISA of HigA2 (left) and HigB2 (right) following induction using IPTG and arabinose, respectively. Black symbols represent absorbance measurements at 450 nm (A450) whereas white and gray symbols represent calculated protein concentration.

IPTG in the 0-100 μM range. Increasing concentration IPTG leads to decrease in sfGFP fluorescence, indicating that HigA2 acts as negative regulator, in line with previous reports (Fig. 4B, upper).⁴⁹ To assess the effect of toxin we performed an experiment with a fixed amount of IPTG (50 μM) to induce HigA2 antitoxin expression and varied the concentration of arabinose between 0 and 100 μM. Increasing arabinose concentration leads to

increase of sfGFP fluorescence indicating de-repression of promoter by HigB2 toxin (Fig. 4B, upper). To verify that the levels of HigA2 and HigB2 change with inducer concentration we performed ELISA on cell lysates and detected proteins using HA-tag and His-tag specific antibodies placed on HigA2 and HigB2, respectively (Fig. 4C). Protein concentrations were calculated from absorbances using a calibration curve of His-GST-HA protein (see Methods and Equation S1, Table S6). Both toxin and antitoxin show concentration-dependent increase, confirming that inducers change the level of proteins in the cell.

A similar setup was applied to the *phd/doc* operon from bacteriophage P1. Doc is a kinase that targets elongation factor Tu⁵⁰, while Phd counteracts its activity by forming an inert complex. Transcription regulation depends on the molar ratio of two proteins through a mechanism known as conditional-cooperativity. In the sub-stoichiometric amounts Doc acts as co-repressor, but when Doc: Phd ratio exceeds 1:1, toxin acts as de-repressor⁵¹. Upon increasing IPTG concentration from 0 to 1000 μ M we observed a decrease of sfGFP fluorescence in line with the proposed repressor activity of Phd (Fig. 4B, lower)^{51,52}. To study the effect of toxin Doc we used a non-toxin variant (H66Y)⁵². At the fixed concentration of IPTG (20 μ M) we varied arabinose concentration from 0 to 10 mM. Initially, we observed a drop in sfGFP fluorescence, but from 0.5 mM arabinose fluorescence intensity increases indicating de-repression (Fig. 4B, lower). Overall, this shows that pRAT-sfGFP vector can be used for studying two-component gene regulatory circuits that respond to the changes in the ratio of two regulators.

Conclusion

Here we present a novel tunable single-vector dual gene expression system pRAT-sfGFP based on the two ubiquitous inducers, arabinose and IPTG. Through appropriate modifications both inducers can separately or in combination produce a tunable and population homogenous expression and show negligible inducer cross-talk. Compared to some other arabinose induced expression systems, it is important to note the transient nature of gene expression in our case, as Tuner[DE3] strain is capable of degrading arabinose. We have designed the pRAT-sfGFP vector where desired genes and operons can be inserted using Golden Gate cloning and tested the systems on prototypical two-component regulatory circuits from bacterial toxin/antitoxin systems. While our vector has a relatively limited range of gene expression, we were able to titrate toxin/antitoxin ratio and measure the regulatory output through reporter protein fluorescence. Compared to other systems, the low-copy number pRAT-sfGFP provides a simpler workflow requiring a single transformation, but still provides gene expression close to physiological levels. The combination of tunable arabinose and IPTG expression in pRAT-sfGFP vector provides a simple and effective tool for *in vivo* study of protein/protein ratio effects on reporter gene expression.

Methods

Plasmids

Vector pET22b(+) containing sfGFP under T7 *lacO* expression control was graciously given by dr. Tomaž Žagar. Scaffold vector, scaffold vector containing HigBA2 system and linear insert containing PhdDoc were obtained from Twist Bioscience (CA, USA). AraE and PhdDoc were inserted into scaffold vector using Golden Gate cloning with *Bsa*I-HF-v2 (NEB, MA, USA)^{53,54}. Vector properties, overhang sequences for Golden Gate cloning and colony PCR results are detailed in supplementary material (Figure S1, Table S1, S2). All constructs were confirmed by sequencing using oligonucleotides and services provided by Eurofins genomics (Ebersberg, Germany). All oligonucleotides were purchased from Integrated DNA Technologies (IDT, Coralville, IA, USA).

Cell growth

Tuner[DE3](Sigma-Aldrich, MA, USA) or Bl21[DE3](Thermo Fisher Scientific, MA, USA) cells were grown overnight in 4–6 mL of minimal media M9 (Table S3–5) with the appropriate antibiotic concentration (50 μ g/mL Kanamycin (Apollo Scientific, Stockport, UK) or 100 μ g/mL Ampicillin (Fisher Scientific, PA, USA)) at 37 °C and constant shaking. Cells were then diluted into fresh minimal media at a ratio of 1:20. After overnight incubation at 18–20 °C 300 μ L of cells per well was transferred into Nunc Multidish 48 plates (Sterile, Non-treated, Thermo Fisher Scientific, MA, USA) or 100 μ L of cells per well into Nunc Microplates for fluorescence-based Assays, 96 well (Non-sterile, Thermo Fisher Scientific, MA, USA). Non-sterile plates were sterilized using 20 min UV-light sterilization prior to use.

We then added appropriate amounts of IPTG (Omnipur IPTG, Sigma-Aldrich, MA, USA) and/or arabinose (L-(+)-arabinose, ≥ 99%, Sigma-Aldrich, MA, USA) to cells in order to induce expression. Induced cells were then incubated at 30 °C with constant shaking.

For the experiment where inducers had different incubation periods, appropriate IPTG concentrations were added to cells grown in the Nunc Multidish 48 prior to second overnight incubation. Following the overnight incubation with IPTG, arabinose was added and cells were then incubated at 30 °C with constant shaking.

Flow cytometry

Cells grown in 48 well plates were diluted to concentrations of approximately 10⁸ cells per mL in phosphate buffer solution (1× PBS, cells diluted 500–4000x) and measured using FACScan flow cytometer (Becton Dickinson, NJ, USA) with a 488 nm excitation laser. Around 30 000–32 000 events were collected at speeds up to 2000 events per second. Flow cytometer measured forward scatter (FSC), side scatter (SSC) and fluorescence data (530/30 nm and 650 LP). Data was analyzed using Flowing Software 2 (Turku Bioscience, Finland). Fluorescence data was gated as depicted in supplementary material (Figure S2).

Plate fluorescence measurements

Fluorescence measurements were performed at 3, 5 and 24 h after induction using microplate reader Infinite Pro 200 (Tecan, Switzerland) or once per hour from 0 to 24 h using BioTek Synergy H1 Multimode Reader (Agilent,

CA, USA). Excitation wavelength was set at 483 nm, emission wavelength was set at 535 nm and Gain was set at 100. Fluorescence was normalized using absorbance measurements at 600 nm (OD₆₀₀).

Immunodetection of HigB2 and HigA2

Cells expressing HigB2 and HigA2 were centrifuged after 24 h of induction and lysed using 2–3 freeze and thaw cycles at -20 °C and room temperature. Cell lysate was centrifuged for 10 min at 10 000 g and 50 µL of supernatant was applied to microplates (F96 MAXISORP Nunc-Immuno Thermo Fisher Scientific, MA, USA). Abundance of His-tagged HigB2 and HA-tagged HigA2 was estimated by quantitative ELISA using mouse Anti-His (MediMabs, Quebec, Canada) or mouse Anti-HA antibodies (Biosensis, Thebarton, Australia) diluted 1:1000 in 1x PBS, 1% milk (Blotting grade, Karlsruhe, Germany), 0,05% Tween20 (for synthesis, Sigma-Aldrich, MA, USA)). HRP-conjugated secondary goat anti-mouse antibodies (ImmunoReagents, NC, USA) were diluted 1:5000 in 1x PBS (1% milk, 0,05% Tween20) and after washing 100 µL of TMB High Sensitivity Substrate Solution was added to well (BioLegend, CA, USA) and incubated for 5–10 min. Reaction was stopped using 100 µL of 0,16 M H₂SO₄ (32%, Sigma-Aldrich, MA, USA) and absorbance was measured at 450 nm and 630 nm using microplate reader BioTek Synergy H1 (Agilent, CA, USA). To estimate HigB2 and HigA2 protein concentrations from the measured absorbance we used a calibration procedure where a known amount of Glutathione S-transferase with N- and C-terminal His and HA tags (purification detailed in supplementary material, Figure S5, S6) was added on the microplate and detected using mouse Anti-His or with Anti-HA antibodies. The obtained calibration curve values (Table S6) were used to estimate concentration of HigB2 and HigA2.

Data availability

The data that support the findings of this study are available in the methods and Supporting Information of this article. Full annotated plasmid sequence for pRAT-sfGFP is also available in Supporting information.

Received: 10 September 2024; Accepted: 16 December 2024

Published online: 02 January 2025

References

1. Makrides, S. C. Strategies for achieving high-level expression of genes in *Escherichia coli*. *Microbiol. Rev.* **60**, 512–538 (1996).
2. Afroz, T., Biliouris, K., Kaznessis, Y. & BeiselC.L. Bacterial sugar utilization gives rise to distinct single-cell behaviours. *Mol. Microbiol.* <https://doi.org/10.1111/mmi.12695> (2014).
3. Bertram, R. & Hillen, W. The application of Tet repressor in prokaryotic gene regulation and expression. *Microb. Biotechnol.* **1**, 2–16 (2008).
4. Schnider-Keel, U. et al. Autoinduction of 2,4-diacetylphloroglucinol biosynthesis in the biocontrol agent *Pseudomonas fluorescens* CHA0 and repression by the bacterial metabolites Salicylate and Pyoluteorin. *J. Bacteriol.* **182**, 1215–1225 (2000).
5. Meyer, A. J., Segall-Shapiro, T. H., Glassey, E., Zhang, J. & Voigt, C. A. *Escherichia coli* Marionette strains with 12 highly optimized small-molecule sensors. *Nat. Chem. Biol.* **15**, 196–204 (2019).
6. Kunjapur, A. M. & Prather, K. L. J. Development of a vanillate biosensor for the vanillin biosynthesis pathway in *E. Coli*. *ACS Synth. Biol.* **8**, 1958–1967 (2019).
7. Parsek, M. R., Val, D. L., Hanzelka, B. L., Cronan, J. E. & Greenberg, E. P. Acyl homoserine-lactone quorum-sensing signal generation. *Proc. Natl. Acad. Sci.* **96**, 4360–4365 (1999).
8. Seo, S. O. & Schmidt-Dannert, C. Development of a synthetic cimate-inducible gene expression system for *Bacillus*. *Appl. Microbiol. Biotechnol.* **103**, 303–313 (2019).
9. Ike, K. et al. Evolutionary Design of Choline-Inducible and -repressible T7-Based induction systems. *ACS Synth. Biol.* **4**, 1352–1360 (2015).
10. Roth, A. & Breaker, R. R. The structural and functional diversity of Metabolite-Binding Riboswitches. *Annu. Rev. Biochem.* **78**, 305–334 (2009).
11. Mandal, M. & Breaker, R. R. Adenine riboswitches and gene activation by disruption of a transcription terminator. *Nat. Struct. Mol. Biol.* **11**, 29–35 (2004).
12. Dixon, N. et al. Reengineering orthogonally selective riboswitches. *Proc. Natl. Acad. Sci.* **107**, 2830–2835 (2010).
13. Binder, D. et al. Homogenizing bacterial cell factories: Analysis and engineering of phenotypic heterogeneity. *Metab. Eng.* **42**, 145–156 (2017).
14. Marschall, L., Sagmeister, P. & Herwig, C. Tunable recombinant protein expression in *E. Coli*: Enabler for continuous processing? *Appl. Microbiol. Biotechnol.* **100**, 5719–5728 (2016).
15. Marschall, L., Sagmeister, P. & Herwig, C. Tunable recombinant protein expression in *E. Coli*: Promoter systems and genetic constraints. *Appl. Microbiol. Biotechnol.* **101**, 501–512 (2017).
16. Kwon, S. K., Kim, S. K., Lee, D. H. & Kim, J. F. Comparative genomics and experimental evolution of *Escherichia coli* BL21(DE3) strains reveal the landscape of toxicity escape from membrane protein overproduction. *Sci. Rep.* **5**, 16076 (2015).
17. Karyolaimos, A., Ampah-Korsah, H., Zhang, Z. & de Gier J.-W. Shaping *Escherichia coli* for recombinant membrane protein production. *FEMS Microbiol. Lett.* **365**, (2018).
18. Kaplan, S., Bren, A., Zaslaver, A., Dekel, E. & Alon, U. Diverse two-dimensional input functions control bacterial sugar genes. *Mol. Cell.* **29**, 786–792 (2008).
19. Novick, A. & Weiner, M. Enzyme induction as an all-or-none phenomenon. *Proc. Natl. Acad. Sci.* **43**, 553–566 (1957).
20. Siegle, D. A. & Hu, J. C. Gene expression from plasmids containing the araBAD promoter at subsaturating inducer concentrations represents mixed populations. *Proc. Natl. Acad. Sci.* **94**, 8168–8172 (1997).
21. Ozbudak, E. M., Thattai, M., Lim, H. N., Shraiman, B. I. & van Oudenaarden A. Multistability in the lactose utilization network of *Escherichia coli*. *Nature* **427**, 737–740 (2004).
22. Fernández-Castané, A., Vine, C. E., Caminal, G. & López-Santín, J. Evidencing the role of lactose permease in IPTG uptake by *Escherichia coli* in fed-batch high cell density cultures. *J. Biotechnol.* **157**, 391–398 (2012).
23. Marbach, A. & Bettenbrock, K. Lac operon induction in *Escherichia coli*: Systematic comparison of IPTG and TMG induction and influence of the transacetylase LacA. *J. Biotechnol.* **157**, 82–88 (2012).
24. Aggarwal, R. K. & Narang, A. Positive feedback exists and drives the glucose-mediated repression in *Escherichia coli*. *Biophys. J.* **121**, 808–819 (2022).
25. Carrier, T. A. & Keasling, J. D. Investigating autocatalytic gene expression systems through mechanistic modeling. *J. Theor. Biol.* **201**, 25–36 (1999).

26. Fritz, G. et al. Single cell kinetics of phenotypic switching in the arabinose utilization system of *E. Coli*. *PLoS One*. **9**, e89532 (2014).
27. Keasling, J. D., Wanner, B. L., Skaug, T., Datsenko, K. A. & Khlebnikov, A. Homogeneous expression of the PBAD promoter in *Escherichia coli* by constitutive expression of the low-affinity high-capacity AraE transporter. *Microbiol. (N Y)*. **147**, 3241–3247 (2001).
28. Chu, I. T., Speer, S. L. & Pielak, G. J. Rheostatic control of protein expression using tuner cells. *Biochemistry* **59**, 733–735 (2020).
29. Afroz, T., Biliouris, K., Boykin, K. E., Kaznessis, Y. & Beisel, C. L. Trade-offs in engineering sugar utilization pathways for titratable control. *ACS Synth. Biol.* **4**, 141–149 (2015).
30. Sagmeister, P., Schimek, C., Meitz, A., Herwig, C. & Spadiut, O. Tunable recombinant protein expression with *E. Coli* in a mixed-feed environment. *Appl. Microbiol. Biotechnol.* **98**, 2937–2945 (2014).
31. Schlegel, S. et al. Optimizing membrane protein overexpression in the *Escherichia coli* strain Lemo21(DE3). *J. Mol. Biol.* **423**, 648–659 (2012).
32. Kim, S. K., Lee, D. H., Kim, O. C., Kim, J. F. & Yoon, S. H. Tunable control of an *Escherichia coli* expression system for the overproduction of membrane proteins by titrated expression of a mutant lac Repressor. *ACS Synth. Biol.* **6**, 1766–1773 (2017).
33. Morra, R. et al. Dual transcriptional-translational cascade permits cellular level tuneable expression control. *Nucleic Acids Res.* **44**, e21–e21 (2016).
34. Dublanche, Y., Michalodimitrakis, K., Küpperer, N., Foglierini, M. & Serrano, L. Noise in transcription negative feedback loops: simulation and experimental analysis. *Mol. Syst. Biol.* **2**, (2006).
35. Nevozhay, D., Adams, R. M., Murphy, K. F., Josić, K. & Balázsi, G. Negative autoregulation linearizes the dose–response and suppresses the heterogeneity of gene expression. *Proc. Natl. Acad. Sci.* **106**, 5123–5128 (2009).
36. Nevozhay, D., Zal, T. & Balázsi, G. Transferring a synthetic gene circuit from yeast to mammalian cells. *Nat. Commun.* **4**, 1451 (2013).
37. Dixon, N. et al. Orthogonal riboswitches for tuneable coexpression in Bacteria. *Angew. Chem. Int. Ed.* **51**, 3620–3624 (2012).
38. Daniel, R., Rubens, J. R., Sarpeshkar, R. & Lu, T. K. Synthetic analog computation in living cells. *Nature* **497**, 619–623 (2013).
39. Silva, J. P. N., Lopes, S. V., Grilo, D. J. & Hensel, Z. Plasmids for independently tunable, low-noise expression of two genes. *mSphere* **4**, (2019).
40. Murakami, M., Murakami, A. M. & Itagaki, S. A dual prokaryotic (*E. coli*) expression system (pdMAX). *PLoS One*. **16**, e0258553 (2021).
41. Lee, S. K. et al. Directed Evolution of AraC for improved compatibility of arabinose- and lactose-inducible promoters. *Appl. Environ. Microbiol.* **73**, 5711–5715 (2007).
42. Shao, B. et al. Single-cell measurement of plasmid copy number and promoter activity. *Nat. Commun.* **12**, 1475 (2021).
43. De Bruyn, P., Girardin, Y. & Loris, R. Prokaryote toxin–antitoxin modules: Complex regulation of an unclear function. *Protein Sci.* **30**, 1103–1113 (2021).
44. Christensen-Dalsgaard, M. & Gerdes, K. Two *higBA* loci in the *Vibrio cholerae* superintegron encode mRNA cleaving enzymes and can stabilize plasmids. *Mol. Microbiol.* **62**, 397–411 (2006).
45. Lehnher, H., Maguin, E., Jafri, S. & Yarmolinsky, M. B. Plasmid addiction genes of bacteriophage P1: doc, which causes cell death on curing of Prophage, and phd, which prevents host death when Prophage is retained. *J. Mol. Biol.* **233**, 414–428 (1993).
46. Hurley, J. M. & Woychik, N. A. Bacterial toxin HigB associates with ribosomes and mediates translation-dependent mRNA cleavage at A-rich sites. *J. Biol. Chem.* **284**, 18605–18613 (2009).
47. Zavrtanik, U., Hadži, S. & Lah, J. Unraveling the thermodynamics of ultra-tight binding of intrinsically disordered proteins. *Front. Mol. Biosci.* **8**, (2021).
48. Hadži, S. et al. Ribosome-dependent *Vibrio cholerae* mRNase HigB2 is regulated by a β-strand sliding mechanism. *Nucleic Acids Res.* **45**, (2017).
49. Hadži, S. et al. Fuzzy recognition by the prokaryotic transcription factor HigA2 from *Vibrio cholerae*. *Nat. Commun.* **15**, 3105 (2024).
50. Castro-Roa, D. et al. The fic protein Doc uses an inverted substrate to phosphorylate and inactivate EF-Tu. *Nat. Chem. Biol.* **9**, 811–817 (2013).
51. Garcia-Pino, A. et al. Allostery and intrinsic disorder mediate transcription regulation by conditional cooperativity. *Cell* **142**, 101–111 (2010).
52. Magnuson, R. & Yarmolinsky, M. B. Corepression of the P1 addiction Operon by Phd and Doc. *J. Bacteriol.* **180**, 6342–6351 (1998).
53. Engler, C. & Marillonnet, S. Golden gate cloning. 119–131(2014). https://doi.org/10.1007/978-1-62703-764-8_9
54. Potapov, V. et al. Comprehensive profiling of four base overhang Ligation Fidelity by T4 DNA ligase and application to DNA assembly. *ACS Synth. Biol.* **7**, 2665–2674 (2018).

Acknowledgements

This work was supported by the Slovenian Research Agency (core funding P1-0201 and grant J1-50026). We acknowledge the support of the Center for Research Infrastructure at the University of Ljubljana, Faculty of Chemistry and Chemical Technology, supported by grant I0-0022 from the Slovenian Research Agency. Z. Ž. acknowledges support through the “Young Researchers” program of the Slovenian Research Agency.

Author contributions

Zala Živič performed experiments and prepared figures and wrote the manuscript. Luka Lipoglavšek edited the manuscript, measured and helped with analysis of Flow Cytometry experiments. Jurij Lah discussed the results and edited the manuscript. San Hadži conceived the study, coordinated the experiments, and wrote the manuscript.

Declarations

Competing interests

The authors declare no competing interests.

Additional information

Supplementary Information The online version contains supplementary material available at <https://doi.org/10.1038/s41598-024-83628-5>.

Correspondence and requests for materials should be addressed to S.H.

Reprints and permissions information is available at www.nature.com/reprints.

Publisher's note Springer Nature remains neutral with regard to jurisdictional claims in published maps and institutional affiliations.

Open Access This article is licensed under a Creative Commons Attribution-NonCommercial-NoDerivatives 4.0 International License, which permits any non-commercial use, sharing, distribution and reproduction in any medium or format, as long as you give appropriate credit to the original author(s) and the source, provide a link to the Creative Commons licence, and indicate if you modified the licensed material. You do not have permission under this licence to share adapted material derived from this article or parts of it. The images or other third party material in this article are included in the article's Creative Commons licence, unless indicated otherwise in a credit line to the material. If material is not included in the article's Creative Commons licence and your intended use is not permitted by statutory regulation or exceeds the permitted use, you will need to obtain permission directly from the copyright holder. To view a copy of this licence, visit <http://creativecommons.org/licenses/by-nc-nd/4.0/>.

© The Author(s) 2024